Table of Contents artwork

Semitransparent superoleophobic coatings with low sliding angles for hot liquids are successfully prepared by fabrication of silica nanotubes on glass slides, and then modification with 1H,1H,2H,2H-perfluorodecyltrichlorosilane.
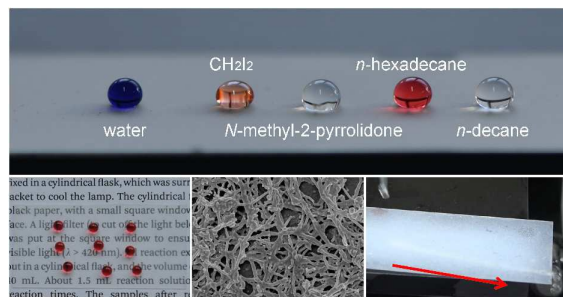
Journal Name

ARTICLE

Semitransparent superoleophobic coatings with low sliding angles for hot liquids based on silica nanotubes

Bucheng Li,[a] Junping Zhang,[*,a] Ziqian Gao,[a] and Qingyun Wei[b]

Semitransparent superoleophobic coatings with low sliding angles for hot liquids are successfully prepared by fabrication of silica nanotubes (SNTs) on glass slides, and then modification with 1*H*,1*H*,2*H*,2*H*-perfluorodecyltrichlorosilane. The SNTs layers are formed by spray-coating a homogeneous dispersion of polydimethylsiloxane (PDMS)-modified multiwalled carbon nanotubes (MWCNTs) onto glass slides followed by calcination to remove MWCNTs, the templates. The successful fabrication of SNTs and the superoleophobic coatings are confirmed with scanning electron microscopy, transmitting electron microscopy, X-ray photoelectron spectroscopy and investigation of the wetting behavior of *n*-decane on the coatings, etc. The microstructures of the SNTs layers have great influences on superoleophobicity of the coatings, which are controllable by simply regulating the diameter of MWCNTs and the concentrations of MWCNTs and PDMS. The superoleophobic coatings feature high contact angles and low sliding angles for various liquids (such as water, toluene, *n*-hexadecane and *n*-decane, etc.), excellent superoleophobicity for hot liquids and good transparency.

1. Introduction

Inspired by the lotus leaf [1] and the leg of water strider [2] in the natural world, superhydrophobic surfaces have generated extensive attention in academic and industrial areas owing to their unique self-cleaning and water-repellent properties.[3-9] It is well known that the combination of proper surface roughness and materials with low surface energy is a successful way to prepare superhydrophobic surfaces.[10-12] On the other hand, superoleophobic surfaces that resist wetting of organic liquids (e.g., alkanes and oils) are also in a high demand in various fields including oil transportation, oil/water separation and microfluidic devices.[13-15] However, it is not so easy to create superoleophobic surfaces because of the low surface tension of most organic liquids, e.g., *n*-hexadecane (27.5 mN/m) and *n*-decane (23.8 mN/m), compared to water (72.8 mN/m).[13, 16] According to the Young's equation, the lower the surface tension, the higher the tendency of a liquid to spread on a solid surface.[17]

Many groups have tried various approaches and techniques to fabricate superoleophobic surfaces on the basis of the experience of designing superhydrophobic surfaces.[18-21] However, most of the reported superoleophobic surfaces are limited to organic liquids with surface tension $\geq$ 27.5 mN/m (*n*-hexadecane). In addition, the droplets of organic liquids often have high contact angles (CAs $\geq$ 150 °) but adhere stably on the surface and cannot roll off, even when

turned upside down.[19-21] In fact, it is very challenging to create superoleophobic surfaces on which the droplets of organic liquids could roll off easily with low sliding angles (SAs) since the interaction between droplets of organic liquids and surfaces should be very weak.[22] Both special microstructure and material of very low surface tension are necessary. Until now, only a few studies achieved superoleophobic surfaces with low SAs for organic liquids with surface tension < 27.5 mN/m by introducing some specially designed patterns like "overhang structures",[23, 24] "re-entrant surface curvatures"[25-29] and intertwined silicone nanofilaments or by using inherently textured fabrics as substrates.[30, 31] Whereas, the fabrication of such microstructures often relies on complicated "etching in" methods (e.g., lithography and anodization) or is limited to particular substrates (e.g., silicon wafer and aluminium foil).

Moreover, in most cases cool liquids (~ 25 ℃) are used to evaluate wettability of superhydrophobic and superoleophobic surfaces. To the best of our knowledge, there are few literatures regarding wettability of superhydrophobic surfaces by hot water ($\geq$ 50 ℃) [32-34] and there is no paper about superoleophobic surfaces with high repellency to hot organic liquids. It was reported that most superhydrophobic surfaces, both natural and artificial, lose superhydrophobicity when exposed to hot water.[32] This is partly because of the condensation of water vapor between the superhydrophobic surface and the hot water droplet, due to their temperature difference, which results in the increase in the liquid-solid contact area.[32] In addition, the decrease of surface tension of water with the increase of temperature also contributes to the loss of superhydrophobicity.[33] However, the real nature for the loss of superhydrophobicity is complicated and still remains open to be studied. Also, superoleophobic surfaces with excellent repellency to hot organic liquids remain to be explored. A superoleophobic surface that can repel hot liquids may have greater potential applications

[a.] *State Key Laboratory for Oxo Synthesis & Selective Oxidation and Center of Eco-material and Green Chemistry Lanzhou Institute of Chemical Physics, Chinese Academy of Sciences, 730000, Lanzhou, P.R. China. E-mail: jpzhang@licp.cas.cn*
[b.] *Department of Chemistry and Environment, Weifang University of Science and Technology, Weifang, 262700, P.R China*
† Electronic Supplementary Information (ESI) available: [TEM, digital and SEM images, surface chemical composition, EDS elemental maps, EDS spectrum and transmittance of the samples and videos]. See DOI: 10.1039/x0xx00000x

such as transportation of hot oil, scalding protection clothes and heat transfer, etc.

Herein, we report a novel templating approach for the fabrication of superoleophobic surfaces by the combination of multiwalled carbon nanotubes (MWCNTs), polydimethylsiloxane (PDMS) and 1*H*,1*H*,2*H*,2*H*-perfluorodecyltrichlorosilane (PFDTCS). For the fabrication of the superoleophobic surfaces in this study, silica nanotubes (SNTs) with different microstructures were formed on glass slides by spray-coating with a homogeneous dispersion of PDMS-modified MWCNTs followed by calcination to remove MWCNTs. Subsequently, the SNTs were modified with PFDTCS to form the superoleophobic SNTs@PFDTCS surfaces. The superoleophobic surfaces feature high CAs and low SAs for various liquids (such as water, toluene, *n*-hexadecane and *n*-decane, etc.), excellent superoleophobicity for hot liquids and good transparency.

2. Experimental

2.1 Materials

MWCNTs 15 nm, 30 nm, 50 nm or 80 nm in average diameter were purchased from Shenzhen Nanotech Port Co., Ltd. The length of MWCNTs is less than 5 μm. Methyltrimethoxysilane (MTMS, 98%) and PFDTCS (97%) were purchased from Gelest. PDMS prepolymer (Sylgard 184A) and the thermal curing agent (Sylgard 184B) were purchased from Dow Corning. Glass slides (24 mm × 50 mm, Menzel, Braunschweig, Germany) were used as the substrates. H_2SO_4, HNO_3, anhydrous ethanol, ammonia (25 wt%), oil red O, methylene blue, diiodomethane, *n*-hexadecane, *n*-dodecane, *n*-decane and toluene were purchased from China National Medicines Co. Ltd. Other reagents used were all of analytical grade. All chemicals were used as received without further purification.

2.2 Preparation of MTMS-modified MWCNTs (M-MWCNTs)

MWCNTs (1.0 g) were treated in 100 mL of concentrated H_2SO_4 and HNO_3 (3:1, v/v) at 60 ℃ for 1 h. 0.5 g of the acid activated MWCNTs and 0.2 mL of MTMS were charged into the mixture of 5 mL of ammonia saturated ethanol solution (3 M) and 5 mL of anhydrous ethanol. The solution was ultrasonicated for 10 min, and then 1.44 g of water was injected quickly into the solution under ultrasonication. After reacting at room temperature under vigorous stirring for 24 h, the M-MWCNTs were washed with 20 mL of ethanol for three times and dried in an oven at 60 ℃.

2.3. Preparation of M-MWCNTs@PDMS coatings

Firstly, a piece of glass slide was cleaned by washing with ethanol, acetone and distilled water in turn, and then dried under a N_2 flow. The M-MWCNTs@PDMS coatings were prepared according to the following procedure. Typically, the spray-coating suspension was prepared by adding 10 mg of M-MWCNTs into 10 mL of *n*-hexane containing PDMS prepolymer (1 mg/mL) and the thermal curing agent (0.1 mg/mL), and then ultrasonicated for 10 min. Subsequently, the suspension was spray-coated onto the vertically placed glass slide using an airbrush (INFINITY 2 in 1, Harder & Steenbeck, Germany) with 0.2 MPa N_2 at a distance of 8 cm. Finally, the coated

glass slide was annealed in an oven at 60 ℃ for 2 h to form the M-MWCNTs@PDMS coating.

2.4 Preparation of SNTs@PFDTCS coatings

M-MWCNTs in the M-MWCNTs@PDMS coating were removed by calcination in air in a muffle furnace at 500 ℃ for 2 h to form the SNTs coating. Subsequently, the SNTs coating was immersed in 60 mL of dry toluene, and then 14 μL of PFDTCS was added. The sample was kept in the above solution for 24 h at room temperature to ensure complete modification of the SNTs. The modified glass slide was washed with 10.0 mL of dry toluene and dried under a nitrogen flow.

2.5 Measurements of CAs and SAs

Measurements of CAs and SAs were performed with a Contact Angle System OCA20 (Dataphysics, Germany) equipped with a tilting table. The syringe was positioned in a way that the liquid droplets (5 μL) could contact surface of the samples before leaving the needle. Tilting angle of the table was adjustable (0 ~ 70 °) and allowed the subsequent measurement of the SAs at the same position on the sample. Because the temperature of liquid droplets decreases quickly, it is difficult to get the real temperature of hot liquid droplets on the coatings. The temperature of hot liquid droplets reported in this paper is the temperature of liquids in the syringe used for measurements of CAs and SAs. The temperature was measured by an IR sensor. In order to reduce thermal loss from the liquid droplets on the coatings, measurements of CAs and SAs were carried out within 5 s of placing the droplets on the coatings. A minimum of six readings were recorded for each sample.

2.6 Characterization

The micrographs of the samples were taken using a field emission scanning electron microscope (SEM, JSM-6701F, JEOL) and a transmitting electron microscope (TEM, TECNAI-G2-F30, FEI). Before SEM observation, all samples were fixed on copper stubs and coated with a layer of gold film (~ 7 nm). The energy dispersive spectroscopy (EDS) analysis was done on the attachment to SEM. For TEM observation, the samples were prepared as follows. A drop of the solution was put on a copper grid and dried in the open atmosphere. The surface chemical composition of the samples was analyzed via X-ray photoelectron spectroscopy (XPS) using a VG ESCALAB 250 Xi spectrometer equipped with a Monochromated AlKa X-ray radiation source and a hemispherical electron analyzer. The spectra were recorded in the constant pass energy mode with a value of 100 eV, and all binding energies were calibrated using the C1s peak at 284.6 eV as the reference. The transmittance of the samples was measured using a UV-Vis spectrophotometer (Specord 200, Analytik Jena AG).
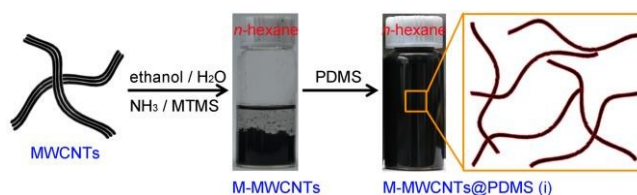

Fig. 1 Schematic illustrations for the preparation of homogeneous dispersion of M-MWCNTs@PDMS in *n*-hexane.

3. Results and discussion

3.1 Design and fabrication of superoleophobic SNTs@PFDTCS coatings

For the fabrication of the superoleophobic SNTs@PFDTCS coatings in this study, a homogeneous dispersion of PDMS-modified MWCNTs (M-MWCNTs@PDMS) in *n*-hexane was prepared in advance (Fig. 1). Subsequently, SNTs with different microstructures were formed on glass slides by spray-coating with the homogeneous dispersion of M-MWCNTs@PDMS followed by calcination to remove MWCNTs. The microstructures of the SNTs coatings are controllable by simply regulating the diameter of MWCNTs (D_{MWCNTs}) and the concentrations of M-MWCNTs ($C_{\text{M-MWCNTs}}$) and PDMS (C_{PDMS}). Finally, the SNTs were modified with PFDTCS in toluene to form the superoleophobic SNTs@PFDTCS coatings.
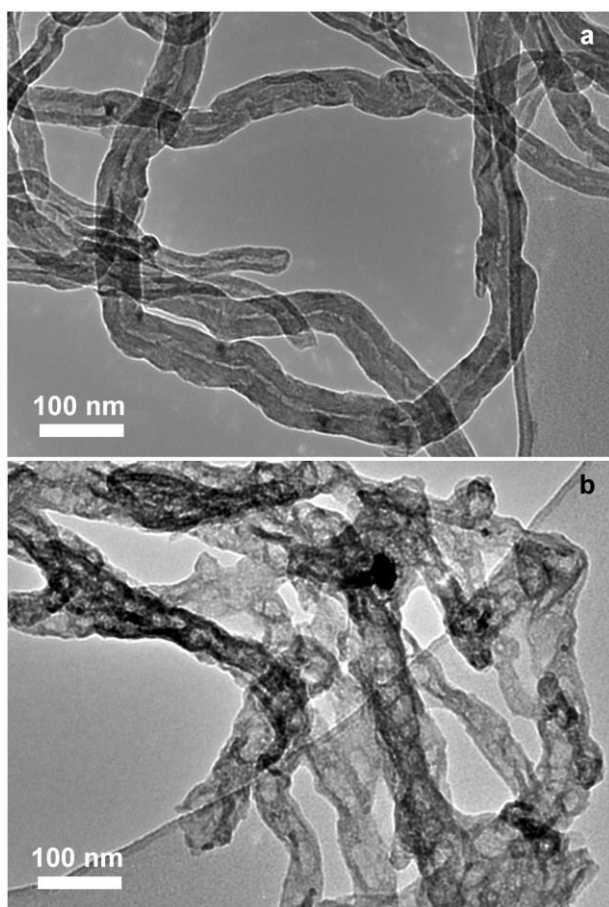

Fig. 2. TEM images of (a) M-MWCNTs@PDMS and (b) SNTs@PFDTCS. $D_{\text{MWCNTs}} = 50$ nm, $C_{\text{M-MWCNTs}} = 1.0$ mg/mL and $C_{\text{PDMS}} = 1.0$ mg/mL.

The homogeneous dispersion of M-MWCNTs@PDMS in *n*-hexane was prepared by modification of acid activated MWCNTs with MTMS via a modified Stöber method,[35] and then mixed with the PDMS prepolymer and the thermal curing agent in *n*-hexane (Fig. 1). The MWCNTs were activated by concentrated H_2SO_4 and HNO_3 (3:1, v/v) at 60 °C to remove impurities. The surface of acid activated MWCNTs is very smooth and no catalyst can be observed (Fig. S1). The dispersibility of M-MWCNTs is poor in *n*-hexane (Figs. 1 and S2). Different from M-MWCNTs, M-

MWCNTs@PDMS is highly dispersible in *n*-hexane. A very homogeneous suspension of M-MWCNTs@PDMS in *n*-hexane, stable over a month, was formed after ultrasonicated for 5 min. It should be noted that both MTMS modification and PDMS are necessary for the fabrication of the homogeneous suspension of M-MWCNTs@PDMS in *n*-hexane. Without MTMS modification, PDMS is not sufficient to disperse MWCNTs very well. MTMS modification and PDMS also provide silicon for the formation of the SNTs in the calcination process.[36] No obvious difference can be seen between acid activated MWCNTs and M-MWCNTs@PDMS via TEM (Figs. S1 and 2a) owing to the very low concentration of PDMS ($C_{\text{PDMS}} = 1.0$ mg/mL).

The uniform black M-MWCNTs@PDMS coatings were prepared simply by spray-coating the homogeneous suspension in *n*-hexane onto glass slides using an airbrush. The random deposition of M-MWCNTs@PDMS generated a crosslinked polymeric network with a rough topography at the surface. M-MWCNTs were cover with a thin layer of PDMS and the space among M-MWCNTs was also filled with PDMS (Fig. 3a). After calcination in air in a muffle furnace at 500 °C for 2 h, the carbonaceous components (MWCNTs, methyl groups of M-MWCNTs and PDMS) in the M-MWCNTs@PDMS coatings were completely removed and the semitransparent SNTs coatings were formed. The silicon for forming the SNTs is from both MTMS and PDMS. The surface roughness increased because of removal of the carbonaceous components in the M-MWCNTs@PDMS coatings. The diameter of SNTs is smaller than that of MWCNTs (Fig. 3b) owing to partial collapse of the PDMS layer on the surface of MWCNTs in the calcination process. Consequently, the tubular structure of MWCNTs is partly preserved according to the TEM image (Fig. 2b). The SNTs coatings are superhydrophilic and superoleophilic. Once the SNTs coatings were immersed in dry toluene that contained PFDTCS, the PFDTCS molecules preferentially anchored onto the hydroxy groups on the surface of SNTs and the SNTs@PFDTCS coatings with a very good superhydrophobicity were created. There was no obvious change of surface morphology after modification with PFDTCS (Fig. 3c).

The surface chemical composition of the M-MWCNTs@PDMS, SNTs and SNTs@PFDTCS coatings was analyzed using XPS analysis (Fig. 4). The C 1s (284.8 eV), O 1s (532.6 eV) and Si 2p (102.3 eV) peaks were detected on the surface of the M-MWCNTs@PDMS coating, indicating the existence of PDMS. All these peaks were also detected in the spectrum of the SNTs coating, but the C 1s peak became very weak and the O 1s peak became very strong owing to removal of MWCNTs and methyl groups of PDMS in the calcination process. The C/O/Si atomic ratio changed from 1:0.43:0.34 to 1:3.24:1.68 after calcination (Table S1). A new intensive F 1s peak (682.6 eV, 49.88 at.%) appeared in the XPS spectrum of the SNTs@PFDTCS coating. In addition, compared to the high-resolution C 1s spectra of the M-MWCNTs@PDMS and SNTs coatings, the new CF_2 (291.3 eV) and CF_3 (293.8 eV) peaks appeared in the C 1s spectrum of the SNTs@PFDTCS coating. These new peaks indicated the successful modification of the SNTs with PFDTCS. The EDS elemental maps of the SNTs@PFDTCS coating confirmed the high uniformity of the coating (Fig. S3) and high F content on the surface (Fig. S4). The perfluoroalkyl group of PFDTCS evidently decreased the surface energy of the SNTs@PFDTCS coating and made the coating superoleophobic.
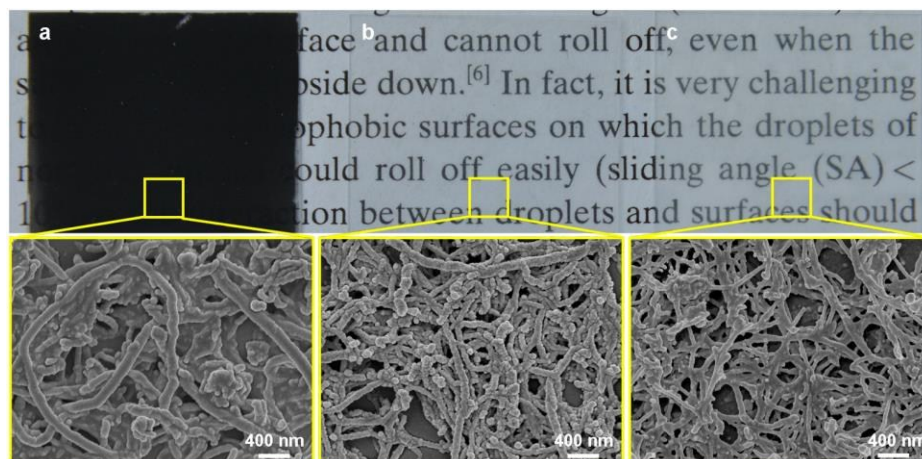
Fig. 3. Digital and SEM images of the (a) M-MWCNTs@PDMS-, (b) SNTs- and (c) SNTs@PFDTCS-coated glass slides. D_{MWCNTs} = 50 nm, $C_{M-MWCNTs}$ = 1.0 mg/mL and C_{PDMS} = 1.0 mg/mL.
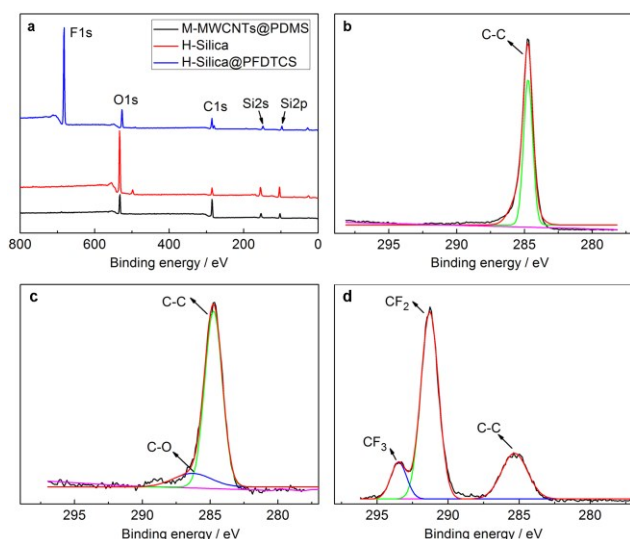

Fig. 4. (a) XPS survey spectra, high-resolution C 1s spectra of (b) M-MWCNTs@PDMS, (c) SNTs and (d) SNTs@PFDTCS coatings. D_{MWCNTs} = 50 nm, $C_{M-MWCNTs}$ = 1.0 mg/mL and C_{PDMS} = 1.0 mg/mL.

3.2 Effects of D_{MWCNTs}, $C_{M-MWCNTs}$ and C_{PDMS} on Wettability and Surface Microstructures

The microstructures of the SNTs coatings have great influences on superoleophobicity of the SNTs@PFDTCS coatings. The microstructures of the SNTs coatings are controllable by simply regulating D_{MWCNTs}, $C_{M-MWCNTs}$ and C_{PDMS}.

The SNTs@PFDTCS coatings showed a perfect superhydrophobicity regardless of D_{MWCNTs}. The CA_{water} and SA_{water} remained almost constant (CA_{water} ~ 158° and SA_{water} ~ 1°) in the range 15 to 80 nm of D_{MWCNTs}. Water droplets are in the Cassie-Baxter state on all the SNTs@PFDTCS coatings. Therefore, D_{MWCNTs} does not have an observable influence on the wetting properties of the coating when water is used as the probe. However, the effect of D_{MWCNTs} is obviously different when n-decane is used as the probe (Fig. 5a). Both $CA_{n-decane}$ and $SA_{n-decane}$ strongly depend on D_{MWCNTs}. When D_{MWCNTs} was small (15 nm and 30 nm), the n-

decane droplets adhered strongly on the SNTs@PFDTCS coatings. A significant increase in the $CA_{n-decane}$ was observed with increasing D_{MWCNTs} to 50 nm; further increase in D_{MWCNTs} to 80 nm slightly increased the $CA_{n-decane}$. A sudden decrease of the $SA_{n-decane}$ to ~8° was observed with increasing D_{MWCNTs} to 50 nm, indicating that the n-decane droplets are in the Cassie-Baxter state. The $SA_{n-decane}$ remained below 10° with further increasing D_{MWCNTs} to 80 nm. It has been shown that the described changes of the $CA_{n-decane}$ and $SA_{n-decane}$ are due to the different D_{MWCNTs}. The SNTs, formed by using MWCNTs as the template, act as a "skeleton" of the superoleophobic coatings. It was found that the behavior of the n-decane droplets on the superoleophobic coatings is closely related to the topography of the skeleton, which can be regulated simply by changing D_{MWCNTs} (Figs. 5b-e and S5). A dense layer of SNTs with a small diameter were formed on the glass slide when D_{MWCNTs} was 15 nm. With increasing D_{MWCNTs} to 30 nm, no obvious change in the surface topography was observed. The surface topography of SNTs obtained under these conditions made the coatings oleophobic with n-decane droplets adhered strongly on the surface. Further increasing D_{MWCNTs} to 50 nm, a dramatic change of surface morphology was observed. The SNTs became very thick and loosely stacked together, which means an evident increase of surface roughness. Such a surface topography could trap more air beneath the n-decane droplets and has successfully made the n-decane droplets in the Cassie-Baxter state. No obvious change could be seen with further increasing D_{MWCNTs} to 80 nm, which is consistent with the changes in the $CA_{n-decane}$ and $SA_{n-decane}$.

$C_{M-MWCNTs}$ has great influences on $CA_{n-decane}$ and $SA_{n-decane}$ of the SNTs@PFDTCS coatings (Fig. 6). The $CA_{n-decane}$ increased significantly from 93° to 154° to with increasing $C_{M-MWCNTs}$ from 0.25 to 1.0 mg/mL, and then remained constant with further increasing $C_{M-MWCNTs}$ to 4.0 mg/mL. When $C_{M-MWCNTs}$ was 0.75 mg/mL, the n-decane droplets adhered strongly on the surface even though the $CA_{n-decane}$ was around 150°, which indicated that the n-decane droplets are in the Wenzel state. This is the frequently observed phenomenon for most of the previously reported superoleophobic coatings.[19-21] The $SA_{n-decane}$ suddenly decreased to 5-8° with increasing $C_{M-MWCNTs}$ to 1.0-2.0 mg/mL, indicating that the n-decane droplets are in the Cassie-Baxter state. Further increase in

$C_{\text{M-MWCNTs}}$ to 4.0 mg/mL results in increase of $SA_{n\text{-decane}}$ to ~12°. It has been mentioned above that the SNTs act as a "skeleton" of the superoleophobic coatings. When $C_{\text{M-MWCNTs}}$ was low, only a small number of SNTs were formed and the surface roughness was low. Thus, the SNTs@PFDTCS coatings are oleophobic. More and more SNTs were formed and the surface roughness increased with increasing $C_{\text{M-MWCNTs}}$ to 1.0-4.0 mg/mL, which made the SNTs@PFDTCS coatings superoleophobic with low $SA_{n\text{-decane}}$.
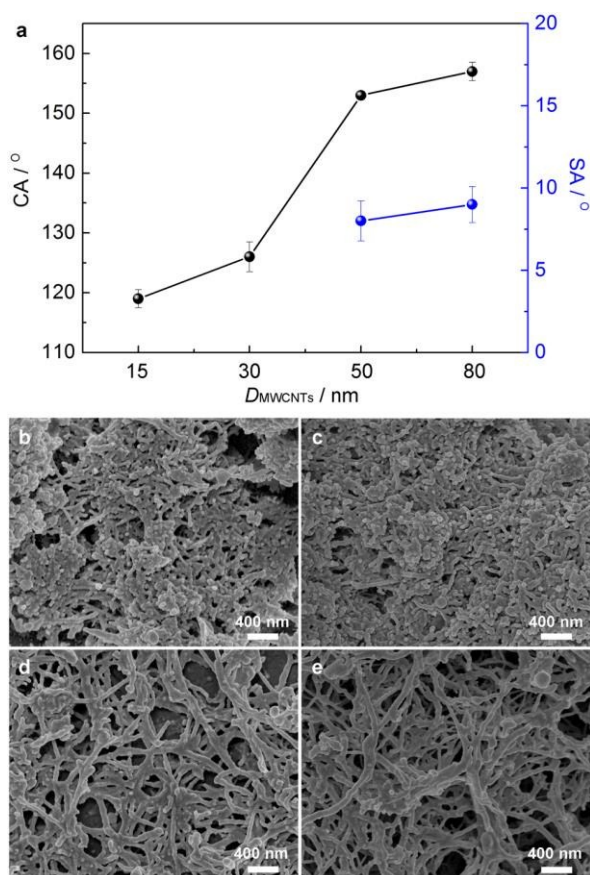

Fig. 5 (a) Variation of $CA_{n\text{-decane}}$ and $SA_{n\text{-decane}}$ of the SNTs@PFDTCS coatings with D_{MWCNTs}, SEM images of the SNTs@PFDTCS coatings prepared with a D_{MWCNTs} of (b) 15 nm, (c) 30 nm, (d) 50 nm and (e) 80 nm. $C_{\text{M-MWCNTs}}$ = 1.0 mg/mL and C_{PDMS} = 1.0 mg/mL.
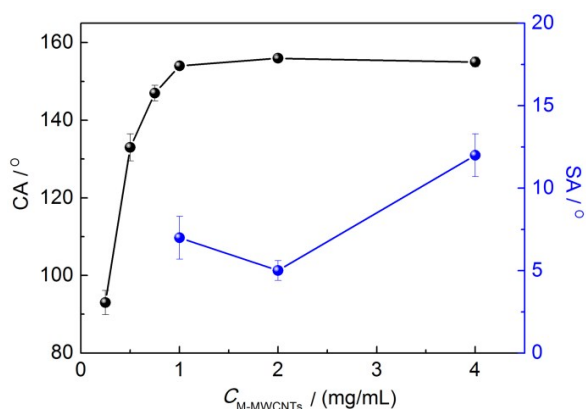

Fig. 6 Variation of $CA_{n\text{-decane}}$ and $SA_{n\text{-decane}}$ of the SNTs@PFDTCS coatings with $C_{\text{M-MWCNTs}}$. D_{MWCNTs} = 50 nm and C_{PDMS} = 1.0 mg/mL.
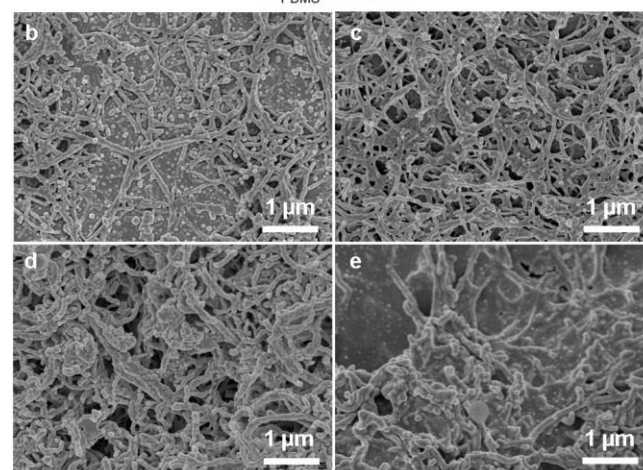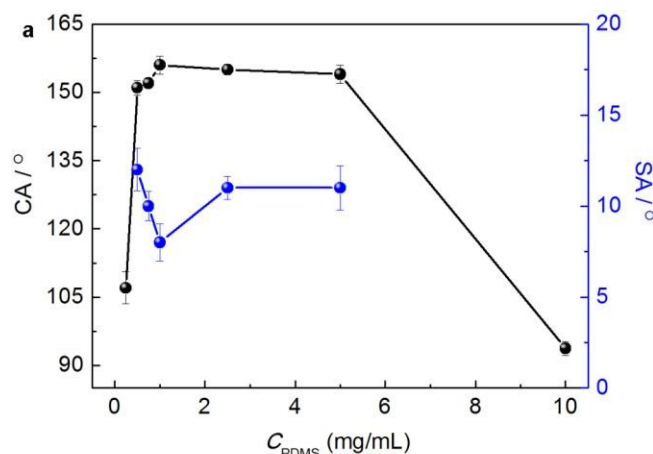
Fig. 7. (a) Variation of $CA_{n\text{-decane}}$ and $SA_{n\text{-decane}}$ of the SNTs@PFDTCS coatings with C_{PDMS}, SEM images of the SNTs@PFDTCS coatings prepared with a C_{PDMS} of (b) 0.25, (c) 1.0, (d) 2.5 and (e) 10.0 mg/mL. D_{MWCNTs} = 50 nm and $C_{\text{M-MWCNTs}}$ = 1.0 mg/mL.

The wettability of the SNTs@PFDTCS coatings also strongly depends on the C_{PDMS} (Fig. 7). The coating was oleophobic with a $CA_{n\text{-decane}}$ of 107° when C_{PDMS} was low (0.25 mg/mL). The $CA_{n\text{-decane}}$ evidently increased to 151° with increasing C_{PDMS} to 0.5 mg/mL and the n-decane droplets could easily roll off the coating with a $SA_{n\text{-decane}}$ of 12°. Further increase in C_{PDMS} to 5.0 mg/mL had no obvious influence on the $CA_{n\text{-decane}}$ and the $SA_{n\text{-decane}}$ remained in the range of 8-11°. However, the $CA_{n\text{-decane}}$ suddenly dropped to 93.7° with increasing C_{PDMS} to 10.0 mg/mL. PDMS is the precursor for the preparation of the SNTs skeleton. The wetting behavior of the n-decane droplets is closely related to the topography of the SNTs skeleton, which can be regulated by changing C_{PDMS} (Fig. 7b-e). Only a small number of SNTs were formed on the glass slide when C_{PDMS} was 0.25 mg/mL, which made the coatings oleophobic. Further increasing C_{PDMS} to 1.0 and 2.5 mg/mL, a dramatic change of surface morphology was observed. The glass slides were covered with a lot of intertwined SNTs with a very rough topography. Such a surface topography has successfully made the coatings superoleophobic with a low $SA_{n\text{-decane}}$. The excess PDMS filled in the space among the MWCNTs and many of the MWCNTs were buried by PDMS when C_{PDMS} was too high (10 mg/mL). Consequently, a surface with lower roughness was formed, which was consistent with the changes in the $CA_{n\text{-decane}}$ and $SA_{n\text{-decane}}$.

Table 1. CAs and SAs of liquids drops (5 μL) of different surface tensions on the SNTs@PFDTCS coating at 25 ℃. D_{MWCNTs} = 50 nm, $C_{M-MWCNTs}$ = 1.0 mg/mL and C_{PDMS} = 1.0 mg/mL.

Liquids	CA / °	SA / °	Surface tension (mN/m, 20 ℃)
water	163.3 ±0.8	1.0 ±0.0	72.8
diiodomethane	158.6 ±1.6	1.8 ±0.9	50.8
N-methyl-2-pyrrolidone	154.1 ±1.3	9.1 ±0.6	40.8
1,2-dichloroethane	154.2 ±0.8	10 ±1.2	33.3
toluene	154.6 ±0.9	6.8 ±0.7	28.4
n-hexadecane	161.4 ±0.5	5.2 ±0.7	27.5
n-dodecane	157.3 ±1.3	6.7 ±1.1	25.4
n-decane	155.3 ±1.7	8.0 ±0.8	23.8

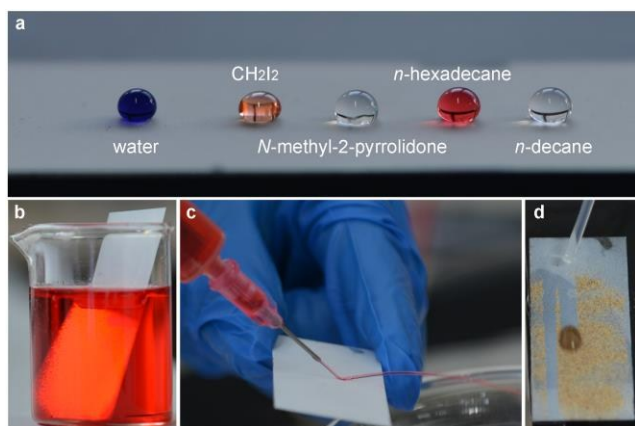### 3.3 Superoleophobicity and transparency of SNTs@PFDTCS coatings

Fig. 8. Images of the SNTs@PFDTCS-coated glass slides (a) with liquids drops of different surface tension, (b) immersed in n-hexadecane, (c) with a jet of n-hexadecane bouncing off and (d) with n-hexadecane to remove the dirt (sand microparticles). D_{MWCNTs} = 50 nm, $C_{M-MWCNTs}$ = 1.0 mg/mL and C_{PDMS} = 1.0 mg/mL.

After confirming the relationship between the preparation parameters (D_{MWCNTs}, $C_{M-MWCNTs}$ and C_{PDMS}), surface topography of the coating and the behavior of n-decane droplets, the superoleophobicity of the SNTs@PFDTCS coatings was tested by recording CAs, SAs and kinetic behaviors of various typical liquids with different surface tension. The CAs and SAs of the liquids on the SNTs@PFDTCS coatings are shown in Table 1. All the liquids investigated, even n-decane, are spherical in shape with high CAs (>154°) and low SAs (<10°) (Fig. 8a). The liquid droplets could easily roll off the 10° tilted SNTs@PFDTCS coatings (Movie S1). This is attributed to the existence of the air cushion between the solid surface and the liquids,[17] and all the liquid droplets are in the

Cassie-Baxter state. The SNTs@PFDTCS coating was reflective in n-hexadecane with a silver mirror-like surface and remained completely dry after taken out, which were direct evidences for the existence of the air cushion (Fig. 8b). This means that most of the area beneath the liquid droplet is a liquid-vapor interface, which indicates that the interaction between the liquid and the coating is very weak. This is also well evidenced by the jetting behavior of n-hexadecane on the SNTs@PFDTCS coating (Fig. 8c). The SNTs@PFDTCS coating also showed self-cleaning property (Fig. 8d and Movie S2). All the liquids listed in Table 1 can be used to efficiently remove powdered dirt on the surface of the coating. This is owing to the weak interaction of the coating with liquid drops and the dirt as well as the rolling motion of liquid drops on the coating.
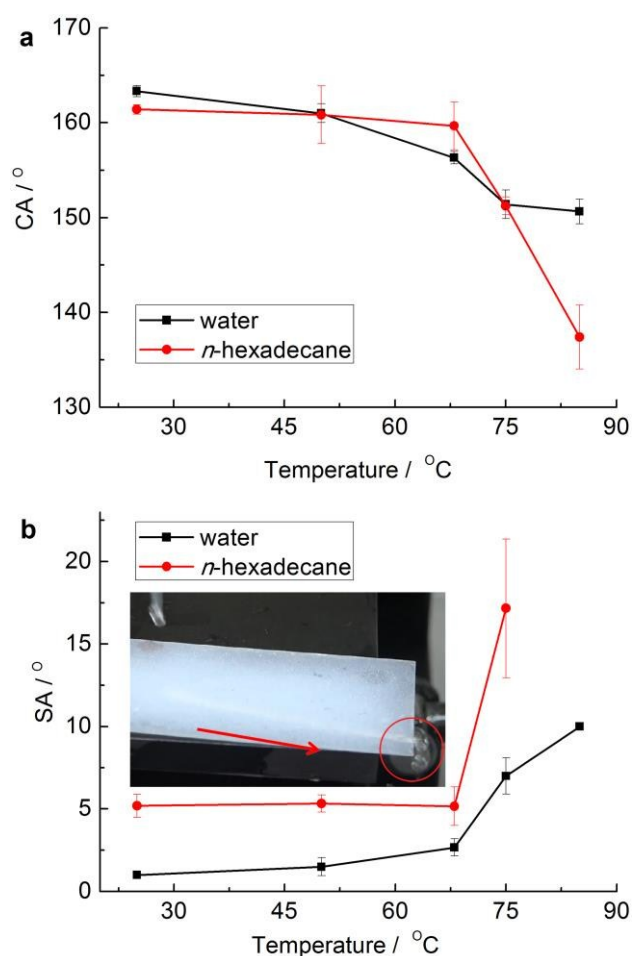

Fig. 9. Variation of (a) CAs and (b) SAs of water and n-hexadecane droplets (8 μL) with their temperature on the SNTs@PFDTCS coating. The inset in (b) shows the path owing to the condensation of water vapor after a hot water drop (75 ℃) rolled off the coating. D_{MWCNTs} = 50 nm, $C_{M-MWCNTs}$ = 1.0 mg/mL and C_{PDMS} = 1.0 mg/mL.

It was reported that most superhydrophobic surfaces, both natural and artificial, lose superhydrophobicity when exposed to hot water.[32] The CA_{water} on lotus leaves dropped drastically to 40° with increasing water temperature to 55 °C.[33] Interestingly, the SNTs@PFDTCS coating showed excellent superoleophobicity not only for liquids at room temperature, but also for hot liquids. The changes of the CAs and SAs of water and n-hexadecane with the

increase of their temperature are shown in Fig. 9. The CA_{water} decreased gradually from 163.3° to 150.6° and the $CA_{n\text{-hexadecane}}$ decreased gradually from 161.4º to 137.4º with the increase of liquid temperature from 25 ℃ to 85 ℃. Meanwhile, the increase of temperature to 68 ℃ had no obvious influence on the SA_{water} and $SA_{n\text{-hexadecane}}$; further increase of the temperature to 75 ℃ resulted in increase of SA_{water} (~7º) and $SA_{n\text{-hexadecane}}$ (~17º). Both the water and n-hexadecane droplets with a temperature of 75 ℃ could still roll off the coating (Movie S3), which means that the hot liquid droplets (75 ℃) are still in the Cassie-Baxter state on the SNTs@PFDTCS coating. When the temperature of liquid droplets increased to 85 ℃, the water droplet could still roll off the coating but the n-hexadecane droplet become sticky on the surface. This means the n-hexadecane droplet has changed from the Cassie-Baxter state to the Wenzel state. The gradual decline of superhydrophobicity and superoleophobicity of the SNTs@PFDTCS coating for hot liquids is because of the condensation of liquid vapor between the coating and the hot liquid droplet, which results in the gradual increase in the liquid-solid contact area.[32] The path owing to the condensation of water vapor after a hot water drop (75 °C) rolled off the coating can be seen clearly (inset in Fig. 9b and Movie S3, part 1). Thus, design of coatings that could reduce the condensation of liquid vapor should be an effective approach to enhance the superoleophobicity for hot liquids. In addition, the decrease of surface tension of liquid with the increase of temperature also contributes to the decline of superhydrophobicity and superoleophobicity.[33] Although gradual decline in the CAs and SAs of water and n-hexadecane were recorded with the increase of their temperature, the SNTs@PFDTCS coating still kept excellent superoleophobicity for hot liquids with temperature up to 75 ℃, which makes the SNTs@PFDTCS coating superior to most of the previously reported natural and artificial superhydrophobic and superoleophobic surfaces.
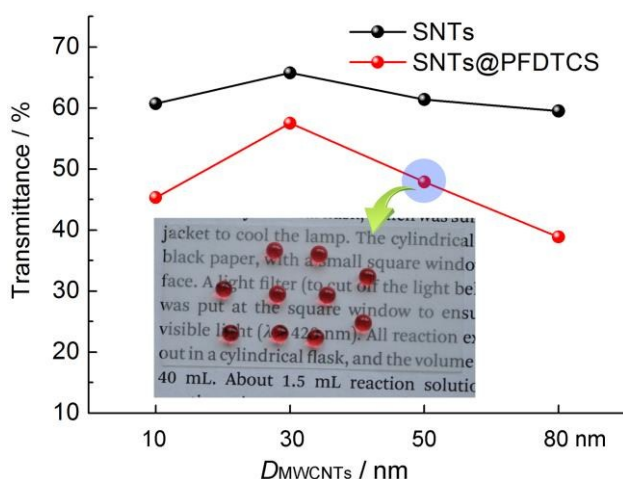

Fig. 10 Variation of transmittance of the SNTs- and SNTs@PFDTCS-coated glass slides at 600 nm with D_{MWCNTs}. The inset is the image of the SNTs@PFDTCS-coated glass slide with 7 μL n-hexadecane droplets (colored with oil red O) on a piece of paper. $C_{M\text{-MWCNTs}}$ = 1.0 mg/mL and C_{PDMS} = 1.0 mg/mL.

The effects of D_{MWCNTs} and subsequent PFDTCS coating could also be seen from changes of the transparency of the SNTs- and SNTs@PFDTCS-coated glass slides (Figs. 10 and S6). With the increase of D_{MWCNTs}, roughness of the SNTs layers increased, and

then a slight decrease of the transmittance was observed. Modification of the SNTs with PFDTCS resulted in a further decrease of the transmittance, but still kept reasonable transparency. Transmittance of the SNTs@PFDTCS-coated glass slide with a D_{MWCNTs} of 50 nm was ~48% at 600 nm. The spray-coating density of M-MWCNTs@PDMS is 1.67 mg/cm^2 on the glass slide (24 mm × 50 mm) and the thickness of the coating is ~9.5 μm. The thickness of the coating can be reduced by decreasing the spray-coating density. The decrease in the spray-coating density could enhance transmittance of the coatings, but resulted in obvious deterioration of the superoleophobicity (Fig. S7). The good transparency is attributed to the uniform SNTs layer which has reduced light scattering. The good transparency of the SNTs@PFDTCS coating is remarkable because superoleophobic coatings have high requirement for surface microstructure, which makes it difficult to give consideration to both superoleophobicity and transparency. Although transparent superhydrophobic surfaces have been extensively studied,[37-42] superoleophobic surfaces with high transparency are rare.[16, 17, 43] The good transparency of the SNTs@PFDTCS coating may expand their possible applications to glass-based substrates.

4. Conclusions

In summary, a simple templating method was developed to generate uniform SNTs layers on glass slides, which have been used as skeletons for successful preparation of semitransparent superoleophobic coatings after modification with PFDTCS. The topography of the SNTs layers plays an important role in influencing superoleophobicity of the coatings and can be regulated simply by D_{MWCNTs}, $C_{M\text{-MWCNTs}}$ and C_{PDMS}. The superoleophobic coatings show high CAs and low SAs for various liquids and good transparency. Moreover, the superoleophobic coatings also show excellent superoleophobicity for hot liquids. We believe that this technique could be used to prepare superoleophobic coatings with controlled topography and the superoleophobic coatings may be applied to various fields. Our primary findings about hot liquid-repellent superoleophobic coatings should be helpful for the further development of this field.

Acknowledgements

Notes and references

1   W. B. C. Neinhuis, *Ann. Bot.*, 1997, **79**, 667-677.
2   X. Gao and L. Jiang, *Nature*, 2004, **432**, 36-36.
3   J. Genzer and K. Efimenko, *Science*, 2000, **290**, 2130-2133.
4   H. Y. Erbil, A. L. Demirel, Y. Avcı and O. Mert, *Science*, 2003, **299**, 1377-1380.
5   N. R. Chiou, C. Lu, J. Guan, L. J. Lee and A. J. Epstein, *Nature Nanotechnol.*, 2007, **2**, 354-357.
6   J. Yuan, X. Liu, O. Akbulut, J. Hu, S. L. Suib, J. Kong and F. Stellacci, *Nature Nanotechnol.*, 2008, **3**, 332-336.

ARTICLE

7   M. Liu, Y. Zheng, J. Zhai and L. Jiang, *Accounts Chem. Res.*, 2009, **43**, 368-377.

8   B. Bhushan and Y. C. Jung, *Prog. Mater. Sci.*, 2011, **56**, 1-108.

9   Y. Lu, S. Sathasivam, J. Song, C. R. Crick, C. J. Carmalt and I. P. Parkin, *Science*, 2015, **347**, 1132-1135.

10   Y. Li, L. Li and J. Sun, *Angew. Chem. Int. Ed.*, 2010, **49**, 6129-6133.

11   S. M. Kang, I. You, W. K. Cho, H. K. Shon, T. G. Lee, I. S. Choi, J. M. Karp and H. Lee, *Angew. Chem. Int. Ed.*, 2010, **49**, 9401-9404.

12   J. P. Zhang and S. Seeger, *Adv. Funct. Mater.*, 2011, **21**, 4699-4704.

13   Z. Chu and S. Seeger, *Chem. Soc. Rev.*, 2014, **43**, 2784-2798.

14   H. Bellanger, T. Darmanin, E. T. de Givenchy and F. Guittard, *Chem. Rev.*, 2014, **114**, 2694-2716.

15   K. Liu, Y. Tian and L. Jiang, *Prog. Mater. Sci.*, 2013, **58**, 503-564.

16   J. P. Zhang and S. Seeger, *Angew Chem Int Ed*, 2011, **50**, 6652-6656.

17   X. Deng, L. Mammen, H. J. Butt and D. Vollmer, *Science*, 2012, **335**, 67-70.

18   A. Steele, I. Bayer and E. Loth, *Nano Lett.*, 2008, **9**, 501-505.

19   H. Li, X. Wang, Y. Song, Y. Liu, Q. Li, L. Jiang and D. Zhu, *Angew. Chem. Int. Ed.*, 2001, **40**, 1743-1746.

20   J. Zimmermann, M. Rabe, G. R. J. Artus and S. Seeger, *Soft Matt.*, 2008, **4**, 450.

21   T. Darmanin and F. d. r. Guittard, *J. Am. Chem. Soc.*, 2009, **131**, 7928.

22   K. Tsujii, T. Yamamoto, T. Onda and S. Shibuichi, *Angew. Chem. Int. Ed.*, 1997, **36**, 1011-1012.

23   L. F. Yuan, T. Z. Wu, W. J. Zhang, S. Q. Ling, R. Xiang, X. C. Gui, Y. Zhu and Z. K. Tang, *J. Mater. Chem. A*, 2014, **2**, 6952-6959.

24   M. Zhang, T. Zhang and T. Cui, *Langmuir*, 2011, **27**, 9295-9301.

25   A. Tuteja, W. Choi, M. Ma, J. M. Mabry, S. A. Mazzella, G. C. Rutledge, G. H. McKinley and R. E. Cohen, *Science*, 2007, **318**, 1618-1622.

26   S. Pan, A. K. Kota, J. M. Mabry and A. Tuteja, *J. Am. Chem. Soc.*, 2013, **135**, 578-581.

27   A. Grigoryev, I. Tokarev, K. G. Kornev, I. Luzinov and S. Minko, *J. Am. Chem. Soc.*, 2012, **134**, 12916-12919.

28   T. Y. Liu and C. J. Kim, *Science*, 2014, **346**, 1096-1100.

29   S. Pechook, N. Kornblum and B. Pokroy, *Adv. Funct. Mater.*, 2013, **23**, 4572-4576.

30   S. Pan, R. Guo and W. Xu, *AIChE J.*, 2014, **60**, 2752-2756.

31   H. Zhou, H. X. Wang, H. T. Niu, J. Fang, Y. Zhao and T. Lin, *Adv. Mater. Interfaces*, 2015, **2**, 1400559.

32   F. Wan, D.-Q. Yang and E. Sacher, *J. Mater. Chem. A*, 2015, **3**, 16953-16960.

33   Y. Liu, X. Chen and J. H. Xin, *J. Mater. Chem.*, 2009, **19**, 5602.

34   Z. J. Yu, J. Yang, F. Wan, Q. Ge, L. L. Yang, Z. L. Ding, D. Q. Yang, E. Sacher and T. T. Isimjan, *J. Mater. Chem. A*, 2014, **2**, 10639-10646.

35   C. H. Xue, P. Zhang, J. Z. Ma, P. T. Ji, Y. R. Li and S. T. Jia, *Chem. Commun.*, 2013, **49**, 3588-3590.

36   Z. Qiang, M. L. Wadley, B. D. Vogt and K. A. Cavicchi, *J. Polym. Sci. B*, 2015, **53**, 1058-1064.

37   J. T. Han, S. Y. Kim, J. S. Woo and G. W. Lee, *Adv. Mater.*, 2008, **20**, 3724-3727.

38   Y. Li, F. Liu and J. Sun, *Chem. Commun.*, 2009, 2730-2732.

39   S. Yu, Z. Guo and W. Liu, *Chem. Commun.*, 2015, **51**, 1775-1794.

40   X. Zhang, H. Kono, Z. Liu, S. Nishimoto, D. A. Tryk, T. Murakami, H. Sakai, M. Abe and A. Fujishima, *Chem. Commun.*, 2007, 4949-4951.

41   G. R. J. Artus, S. Jung, J. Zimmermann, H. P. Gautschi, K. Marquardt and S. Seeger, *Adv. Mater.*, 2006, **18**, 2758-2762.

42   J. Li, L. Li, X. Du, W. Feng, A. Welle, O. Trapp, M. Grunze, M. Hirtz and P. A. Levkin, *Nano Lett.*, 2015, **15**, 675-681.

43   S. E. Lee, H.-J. Kim, S.-H. Lee and D.-G. Choi, *Langmuir*, 2012, **29**, 8070-8075.